RL-TR-92-258
In-House Report
September 1992

ADAPTIVE NULLING IN HYBRID REFLECTOR ANTENNAS

Robert A. Shore

APPROVED FOR PUBLIC RELEASE; DISTRIBUTION UNLIMITED.

Rome Laboratory
Air Force Systems Command
Griffiss Air Force Base, New York

This report has been reviewed by the Rome Laboratory Public Affairs Office (PA) and is releasable to the National Technical Information Service (NTIS). At NTIS it will be releasable to the general public, including foreign nations.

RL-TR-92-258 has been reviewed and is approved for publication.

APPROVED:

DANIEL J. JACAVANCO
Chief, Antenna Systems Branch
Antennas & Components Division
Electromagnetics & Reliability Directorate

FOR THE COMMANDER:

JOHN K. SCHINDLER, Director
Electromagnetics & Reliability Directorate

If your address has changed or if you wish to be removed from the Rome Laboratory mailing list, or if the addressee is no longer employed by your organization, please notify RL(ERAS) Hanscom AFB MA 01731-5000. This will assist us in maintaining a current mailing list.

Do not return copies of this report unless contractual obligations or notices on a specific document require that it be returned.

REPORT DOCUMENTATION PAGE

Form Approved
OMB No. 0704-0188

1. AGENCY USE ONLY (Leave blank)	2. REPORT DATE	3. REPORT TYPE AND DATES COVERED
	September 1992	In-House 9/90 - 8/92

4. TITLE AND SUBTITLE
Adaptive Nulling in Hybrid Reflector Antennas

5. FUNDING NUMBERS
PE: 62702F
PR: 4600
TA: 15
WU: 07

6. AUTHOR(S)
Robert A. Shore

7. PERFORMING ORGANIZATION NAME(S) AND ADDRESS(ES)
Rome Laboratory/ERAS
Hanscom AFB, MA 01731-3010

8. PERFORMING ORGANIZATION REPORT NUMBER
RL-TR-92-258

9. SPONSORING/MONITORING AGENCY NAME(S) AND ADDRESS(ES)

10. SPONSORING/MONITORING AGENCY REPORT NUMBER

11. SUPPLEMENTARY NOTES
This project was funded in part by the Laboratory Director's Independent Research Program.

12a. DISTRIBUTION/AVAILABILITY STATEMENT
Approved for public release; Distribution unlimited

12b. DISTRIBUTION CODE

13. ABSTRACT (Maximum 200 words)

Hybrid antennas, the combination of a radiating or receiving aperture with an array feed, have been the subject of considerable recent interest because they offer some of the versatility of phased array antennas at a much lower cost. Adaptive nulling in hybrid antennas has not received as much attention as other important aspects, such as compensation for reflector surface distortion, scanning, pattern calculation, and the design of multibeam antennas. In this report we investigate adaptive nulling in hybrid reflector antennas using the Generalized Sidelobe Canceller algorithm. A general framework is presented for the computer simulation of narrow band adaptive nulling in hybrid reflector antennas that takes account of the details of reflector scattering and polarization. The general framework is then illustrated by the results of calculations performed for an offset paraboloid with a planar feed located in the focal plane of the paraboloid.

14. SUBJECT TERMS			15. NUMBER OF PAGES
Hybrid antennas	Adaptive nulling	Reflectors	44
Offset paraboloid	Array feed	Generalized sidelobe	16. PRICE CODE
canceller			

17. SECURITY CLASSIFICATION OF REPORT	18. SECURITY CLASSIFICATION OF THIS PAGE	19. SECURITY CLASSIFICATION OF ABSTRACT	20. LIMITATION OF ABSTRACT
UNCLASSIFIED	UNCLASSIFIED	UNCLASSIFIED	SAR

Contents

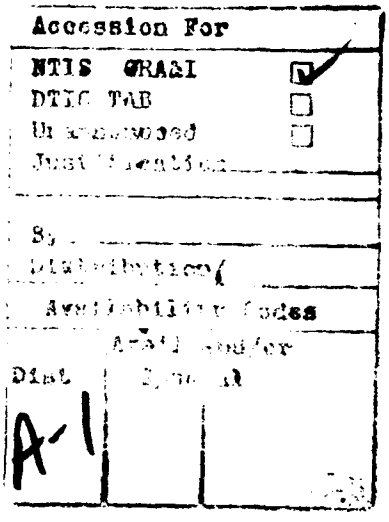

Illustrations

Adaptive Nulling in Hybrid Reflector Antennas

1. INTRODUCTION

Hybrid antennas, the combination of an array antenna with a radiating or receiving aperture, have been the subject of considerable attention in recent years. A basic review of the subject has been written by Mailloux.[1] The interest in hybrid antennas is due in large part to the fact that they can offer some of the versatility (pattern control, rapid scanning) of phased array antennas at a much lower cost than that of phased array antennas.

The literature on hybrid antennas has extensively treated a number of important topics. Thus, for example, array feeds have been investigated for correcting reflector surface distortion,[2,3,4,5] for scanning,[6,7,8,9,10,11] and for designing multiple beam antennas.[12,13,14,15,16]

Received for Publication 18 September 1992

1 Mailloux, R.J. (1982) Hybrid antennas, *The Handbook of Antenna Design*, Vol. 1, A.W. Rudge et al, Eds., Peter Peregrinus, Ltd., London, Chap. 5.

2 Rudge, A.W., and Davies, D.E. (1970) Electronically controllable primary feed for profile-error compensation of large parabolic reflectors, *IEE Proc.*, **117**:351-358.

3 Blank, S.J., and Imbriale, W.A. (1988) Array feed synthesis for correction of reflector distortion and vernier beamsteering, *IEEE Trans. Antennas Propagat.*, **36**:1351-1358.

4 Cherrette, A.R., et al (1989) Compensation of reflector antenna surface distortion using an array feed, *IEEE Trans. Antennas and Propagat.*, **37**:966-978.

The radiation patterns of reflector antennas with array feeds have also been the subject of considerable study,[17,18,19,20,21,22,23,24,25,26] To date, however, relatively little has been published

---

[5] Rahmat-Samii, Y. (1990) Array feeds for reflector surface distortion compensation: concepts and implementation, *IEEE Antennas and Propagat. Magazine*, **32**:(No. 4)20-26.

[6] Fante, R.L. (1980) Systems study of overlapped subarrayed scanning antennas, *IEEE Trans. Antennas Propagat.*, **AP-28**:668-679.

[7] Mrstik, A.V., and Smith, P.G. (1981) Scanning capabilities of large parabolic cylinder reflector antennas with phased-array feeds, *IEEE Trans. Antennas Propagat.*, **AP-29**:455-462.

[8] Hung, C.C. and Mittra, R. (1983) Secondary pattern and focal region distribution of reflector antennas under wide-angle scanning, *IEEE Trans. Antennas Propagat.*, **AP-31**:756-763.

[9] Rinous, P.J., et al (1983) The analysis of hybrid reflector antennas, *Third International Conference on Antennas and Propagation ICAP 83*, pp. 318-321.

[10] O'Brien, M.J., and Shore, R.A. (1984) Paraboloid scanning by array feeds: a low sidelobe synthesis technique, *IEEE AP-S International Symposium, 1984 International Symposium Digest, Antennas and Propagation, Vol. I*, pp. 272-275.

[11] Pearson, R.A., et al (1986) Electronic beam scanning using an array-fed dual offset reflector antenna, *IEEE AP-S International Symposium, 1986 International Symposium Digest, Antennas and Propagation, Vol. I*, pp. 263-266.

[12] Scott, W.G., et al (1977) Design tradeoffs for multibeam antennas in communication satellites, IEEE Communications Society Magazine, **15**:(No. 2)9-15.

[13] Bird, T.S. (1982) Contoured-beam synthesis for array-fed reflector antennas by field correlation, *IEE Proc.*, 129:(Pt. H)293-298.

[14] Ricardi, L.J. (1982) Multiple beam antennas, *The Handbook of Antenna Design, Vol. 1*, A.W. Rudge et al, Eds., Peter Peregrinus, Ltd., London, Chap. 6.

[15] Balling, P. (1987) Spacecraft multi-beam and contoured-beam antennas, *AGARD Lecture Series No. 151, Microwave Antennas for Avionics.*

[16] Adatia, N., et al (1989) Multicoverage shaped reflector antenna designs, *IEEE International Symposium, 1989 International Symposium Digest, Antennas and Propagation, Vol. 3*, pp. 1182-1186.

[17] Bird, T.S., and Boomars, J.L. (1980) Evaluation of focal fields and radiation characteristics of a dual-offset reflector antenna, *IEE Proc.*, **127**:(Pt. H)209-218.

[18] Hsaio, J.K. (1983) *A FORTRAN Computer Program to Compute the Radiation Pattern of an Array-Fed Paraboloidal Reflector*, Naval Research Laboratory Report 8740.

[19] Morris, G. (1984) Receiving analysis of the shaped cylindrical reflector antenna with an array feed, *IEE Proc.*, **131**:(Pt. H)123-125.

[20] Steyskal, H. and Shore, R.A. (1984) *Efficient Computation of Reflector Antenna Aperture Distributions and Far Field Patterns*, Rome Air Development Center Rept. RADC-TR-84-45, Available from National Technical Information Service (NTIS) AD A143319.

[21] Jong, H.Y., et al (1984) Analysis of paraboloidal reflector fields under oblique incidence, *IEEE International Symposium, 1984 International Symposium Digest, Antennas and Propagation*, Vol. 1, pp. 305-308.

[22] Clarricoats, P.J.B., et al (1984) Effects of mutual coupling in conical horn arrays, *IEE Proc.*, **131**:(Pt. H)165-171.

on the important topic of adaptive nulling with hybrid antennas. Chadwick et al[27,28] have described an adaptive reflector system claimed to be capable of nulling a large number of simultaneous broad bandwidth interferers with arbitrary polarization. Their technique utilizes an adaptive array feed located in the focal plane of a Cassegrain or prime focus fed reflector. Their published results are somewhat general in nature and do not go into much detail concerning either the analysis and computer simulation of the system, or the implementation of their system in a test design. Mayhan in his work on multiple beam antennas (MBA) for communication systems[29,30,31] has discussed adaptive nulling in a generic MBA system with idealized beams. His work, though certainly applicable to hybrid antennas generally, does not address the details of reflector scattering and polarization, which play a very important role in adaptive nulling in hybrid reflector antennas.

One reason for the small published literature on adaptive nulling in hybrid antennas may be that much of the work performed on the subject has been proprietary. Another reason may be that no special adaptive nulling techniques are required for hybrid antennas. Existing adaptive nulling techniques developed for array antennas can in principle be directly applied to hybrid antennas as well. Nevertheless, it is worthwhile to investigate the details of adaptive nulling in hybrid antennas as a way of providing designers of adaptive hybrid antennas important information about the parameters affecting their performance. The analytic and computational effort required to simulate adaptive hybrid antennas is considerable and this also may account for the scarcity of published results.

In this report we consider adaptive nulling in hybrid reflector antennas. A hybrid antenna here consists of a reflector (single or multiple) combined with a feed array. A narrow band system is assumed. It is also assumed that the signals received from the elements from the

---

[23] Clarricoats, P.J.B., et al (1984) Performance of offset reflector antennas with array feeds. *IEE Proc.*, **131**:(Pt. H)172-178.

[24] Lam, P.T., et al (1985) Directivity optimization of a reflector antenna with cluster feeds: a closed form solution, *IEEE Trans. Antennas Propagat.*, **AP-33**:1163-1174.

[25] Rusch, W.V.T., and Prata, A. (1990) *Computation of Focal-Region Fields of Offset Dual Reflector Antennas for Scanning Applications*, Rome Air Development Center Rept. RADC-TR-90-299, AD B153991L.

[26] Rusch, W.V.T., and Prata, A. (1991) *Efficient Computation of Classical Offset Dual Reflector Antennas Excited by Array Feeds*, Rome Laboratory Rept. RL-TR-91-7, AD B154936L.

[27] Chadwick, G.G., et al (1980) Adaptive antenna/receiver-processor system, *Proceedings of the 1980 Antenna Applications Symposium, Robert Allerton Park, University of Illinois.*

[28] Chadwick, G.G., et al (1981) Adaptive antenna/receiver processor system, *IEEE-AP-S-International Symposium, 1981 International Symposium Digest, Antennas and Propagation*, Vol. I, pp. 272-275.

[29] Mayhan, J.T. (1976) Nulling limitations for a multiple-beam antenna, *IEEE Trans. Antennas Propagat.*, **AP-24**:769-779.

[30] Mayhan, J.T. (1978) Adaptive nulling with multiple-beam antennas, *IEEE Trans. Antennas Propagat.*, **AP-26**:267-273.

[31] Mayhan, J.T. (1979) Some techniques for evaluating the bandwidth characteristics of adaptive nulling systems, *IEEE Trans. Antennas Propagat.*, **AP-27**:363-373.

array feed can be weighted in both amplitude and phase and then summed to form the array output. The particular adaptive nulling algorithm used in this study is the Generalized Sidelobe Canceller (GSC) due to Griffiths et al.[32,33,34] It was found that the flexibility and conceptual clarity offered by this algorithm made it particularly attractive for use here.

Section 2 reviews the GSC algorithm. Section 3 presents a general framework for treating adaptive nulling in array-fed reflectors. Section 4 discusses how the computations were performed for a particular hybrid antenna configuration, an offset paraboloidal reflector with an array feed in the focal plane. Section 5 concludes by showing and discussing the results of calculations performed to illustrate the general theory.

2. THE GENERALIZED SIDELOBE CANCELLER

The adaptive nulling scheme used in this study, known as the Generalized Sidelobe Canceller (GSC), was developed by Griffiths et al.[32,33,34] The structure of the GSC is shown in Figure 1. The complex vector $\underline{x}(n)$, the array data vector, is the nth time sample of signals from the N array elements. It contains the desired signal as well as internal noise and external interference. The vector of complex weights of dimension N, $\underline{w}_{ql}$, is the quiescent weight vector that defines the array response when the array data vector consists of uncorrelated noise only. The signal, $y_q(n)$, resulting from weighting the array data vector by the quiescent weight vector, is given by

$$y_q(n) = \underline{w}_{ql}^T \underline{x}(n) \tag{1}$$

where T denotes the transpose of a vector. Griffiths has shown[34] that the quiescent weight vector can be obtained from

---

[32] Jim, C.W. (1977) A comparison of two LMS constrained optimal array structures, *Proc. IEEE*, **65**:1730-1731.

[33] Griffiths, L.J., and Jim, C.W. (1982) An alternative approach to linearly constrained adaptive beamforming, *IEEE Trans. Antennas Propagat.*, **AP-30**:27-34.

[34] Griffiths, L.J., and Buckley, K.M. (1987) Quiescent pattern control in linearly constrained adaptive arrays, *IEEE Trans. Acoustics, Speech, and Signal Processing*, **ASSP-35**:917-926.

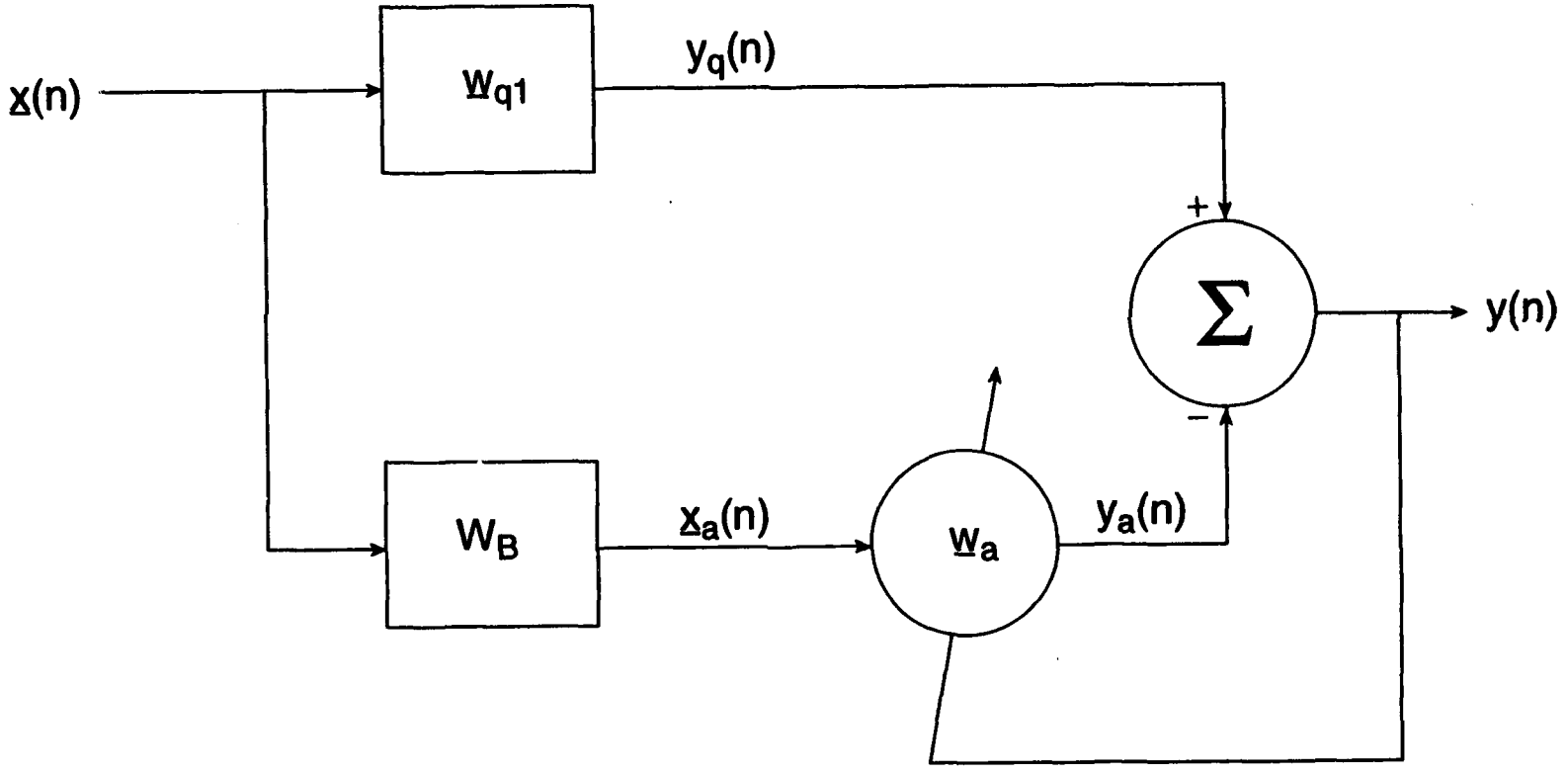

Figure 1. Block Diagram of the Generalized Sidelobe Canceller.

$$\underline{w}_{ql} = \left[I - C\left(C^{\dagger}C\right)^{-1} C^{\dagger}\right]\underline{w}_0 + \underline{w}_q \tag{2a}$$

where

$$\underline{w}_q = C\left(C^{\dagger}C\right)^{-1} \underline{g}\,. \tag{2b}$$

In Eq. (2), I is the N x N identity matrix, $\underline{w}_0$ is the set of weights that corresponds to a desired or design array pattern (for example, a low sidelobe pattern with mainbeam pointing in a specified direction), and † denotes the conjugate transpose of a matrix. C is the N x M constraint matrix which, via the constraint equation (the matrix representation of M constraints)

$$C^{\dagger}\underline{w} = \underline{g} \tag{3}$$

is used to specify that a set of array weights $\underline{w}$ shall result in a pattern with, say, a given mainbeam and nulls in a given set of directions. The elements of each of the M rows of $C^{\dagger}$ are simply the outputs of the respective array elements in response to a plane wave of unit amplitude and specified polarization incident on the antenna from a particular direction, and the corresponding element of the constraint vector $\underline{g}$ is the value that the array output is required to have when the antenna is so illuminated. An alternative, and simpler to calculate, expression for $\underline{w}_{ql}$ is given in Section 3.

The N x [N – (M + 1)] matrix W_B is known as the blocking matrix. It is formed by satisfying two conditions: (1) the columns of W_B are linearly independent, and (2)

$$\left[C \mid \underline{w}_1\right]^{\dagger} W_B = 0 \tag{4}$$

where

$$\underline{w}_1 = \underline{w}_{ql} - \underline{w}_q \tag{5}$$

and 0 is a matrix of zeros of dimension $(M + 1) \times [N - (M + 1)]$. Thus each column of W_B is orthogonal to each column of $[C|\underline{w}_1]$. (The reason for appending the additional column $\underline{w}_1$ to the constraint matrix C is, as Griffiths has shown,[34] to force the quiescent array response to correspond to the set of weights $\underline{w}_{ql}$ that satisfies the constraints and minimizes the squared difference $|\underline{w}_{ql} - \underline{w}_0|^2$ with the set of design weights $\underline{w}_0$. If the column $\underline{w}_1$ is not appended to the constraint matrix, the quiescent response of the GSC will be given by $\underline{w}_q$ of Eq. (2b), the set of weights that satisfies the constraints and minimizes the array output power, even though $\underline{w}_{ql}$ is used in the upper path of the GSC. This quiescent response will then not have the desired features of the design pattern such as low sidelobes. By adding only one additional constraint to the system, the quiescent response can thus be made to closely resemble any design pattern, a remarkable result.) Since M + 1 degrees of freedom are used to satisfy the constraints, there are N – (M + 1) degrees of freedom remaining that can be used for adaptive nulling.

The output vector from the blocking matrix (see Figure 1)

$$\underline{x}_a(n) = W_B^T \underline{x}(n), \tag{6}$$

a vector of dimension N – (M + 1), is then multiplied by the vector of adapted weights, $\underline{w}_a$, and the adapted weights are determined by requiring that the resulting output

$$y_a(n) = \underline{w}_a^T \underline{x}_a(n) \tag{7}$$

be as close as possible in a least mean square (LMS) sense to the output $y_q(n)$ of the quiescent beamformer given by Eq. (1). The well-known solution to the LMS optimization is given by[35]

$$\underline{w}_a = R_{\underline{x}_a \underline{x}_a}^{-1} \underline{r}_{\underline{x}_a y_q} \tag{8}$$

where $R_{\underline{x}_a \underline{x}_a}$ is the covariance matrix given by

$$R_{\underline{x}_a \underline{x}_a} = \overline{x_a^* x_a^T}, \tag{9}$$

---

[35] Widrow, B., et al (1967) Adaptive antenna systems, *Proc. IEEE*, **55**:2143-2159.

$$r_{\underline{x}_a y_q} = \overline{\underline{x}_a^* y_q} \,, \tag{10}$$

and the bar over a quantity denotes the time average. Substituting Eq. (6) into Eq. (9),

$$R_{\underline{x}_a \underline{x}_a} = \overline{\left(W_B^T \underline{x}\right)^* \left(W_B^T \underline{x}\right)^T}$$

$$= W_B^\dagger \overline{\underline{x}^* \underline{x}^T} W_B$$

$$= W_B^\dagger R_{\underline{x}\underline{x}} W_B \tag{11}$$

and substituting Eqs. (1) and (6) into Eq. (10)

$$r_{\underline{x}_a y_q} = \overline{\left(W_B^\dagger \underline{x}^*\right)\left(\underline{x}^T \underline{w}_{ql}\right)}$$

$$= W_B^\dagger R_{\underline{x}\underline{x}} \underline{w}_{ql} \tag{12}$$

so that from Eq. (8)

$$\underline{w}_a = \left(W_B^\dagger R_{\underline{x}\underline{x}} W_B\right)^{-1} W_B^\dagger R_{\underline{x}\underline{x}} \underline{w}_{ql}. \tag{13}$$

The vector of effective weights of the GSC is given by

$$\underline{w} = \underline{w}_{ql} - W_B \underline{w}_a \tag{14}$$

and the array output by

$$y(n) = (\underline{w}_{q1} - W_B \underline{w}_a)^T \underline{x}(n) . \tag{15}$$

We see from Eq. (13) that if the array data vector, $\underline{x}$, consists of uncorrelated noise so that $R_{\underline{x}\underline{x}} = I$, then

$$\underline{w}_a = \left(W_B^\dagger W_B\right)^{-1} W_B^\dagger \underline{w}_{q1}$$

$$= \left(W_B^\dagger W_B\right)^{-1} W_B^\dagger \left(\underline{w}_1 + \underline{w}_q\right). \tag{16}$$

But from Eq. (4)

$$W_B^\dagger \underline{w}_1 = 0_{N-(M+1)} \tag{17}$$

and from Eqs. (2) and (4)

$$W_B^\dagger \underline{w}_q = 0_{N-(M+1)} \tag{18}$$

where $0_{N-(M+1)}$ is a column vector consisting of $N - (M + 1)$ zeros, so that the adapted weight vector is zero. Hence, when the array data vector consists of uncorrelated noise the quiescent array response is obtained.

It should be noted in relation to Eq. (13) that although in theory the matrix $W_B^\dagger R_{\underline{x}\underline{x}} W_B$ is non-singular and so invertible, in practice it can be highly ill-conditioned, thus making Eq. (13) an unreliable way of computing the adaptive weights. An alternative equation can then be used to calculate the vector $\underline{w}$ of effective weights for the GSC [32,34], namely

$$\underline{w} = R_{\underline{x}\underline{x}}^{-1} C' \left(C'^\dagger R_{\underline{x}\underline{x}}^{-1} C'\right)^{-1} C'^\dagger \underline{w}_{q1} \tag{19}$$

where C' is the constraint matrix C with the vector $\underline{w}_1$ appended (see Eq. (4))

$$C' = [C \mid \underline{w}_1] . \tag{20}$$

3. ADAPTIVE NULLING WITH ARRAY-FED REFLECTORS

In this section we apply the framework of the GSC presented in Section 2 to adaptive nulling with array-fed reflectors. We keep the discussion as general as possible so that it is applicable to any array or array-fed antenna. The notation used is consistent with that used in Section 2.

Consider an array feed of N elements and let $e_{\theta i}(\theta, \phi)$, $e_{\phi i}(\theta, \phi)$, $i = 1, 2, \ldots N$, be the output of the ith element of the feed array in response, respectively, to a unit amplitude θ- or ϕ-electrically polarized plane wave incident on the antenna. A global cartesian coordinate system, and associated spherical coordinate system, is assumed. Also, assume a set of feed array weights, w_{0i}, $i = 1, 2, \ldots N$, designed to yield a desired (design) antenna pattern; for example, a pattern with low sidelobes and mainbeam pointing in the direction (θ_0, ϕ_0). The corresponding receive antenna patterns are then denoted by

$$f_{0\theta}(\theta, \phi) = \sum_{i=1}^{N} w_{0i}\, e_{\theta i}(\theta, \phi) \tag{21a}$$

$$f_{0\phi}(\theta, \phi) = \sum_{i=1}^{N} w_{0i}\, e_{\phi i}(\theta, \phi). \tag{21b}$$

By reciprocity, the transmit antenna pattern corresponding to complex excitations w_{0i} of the N feed array elements is given by

$$\underline{f}_0(\theta, \phi) = f_{0\theta}(\theta, \phi)\,\hat{\theta} + f_{0\phi}(\theta, \phi)\,\hat{\phi}$$

$$= \sum_{i=1}^{N} w_{0i}\left[e_{\theta i}(\theta, \phi)\,\hat{\theta} + e_{\phi i}(\theta, \phi)\,\hat{\phi}\right]. \tag{22}$$

Now suppose that deterministic nulls for arbitrarily polarized incoming plane waves are desired in the directions (θ_k, ϕ_k), $k = 1, 2, \ldots, K$, while keeping the antenna pattern as close as possible to $f_{0\theta}(\theta, \phi)$ and $f_{0\phi}(\theta, \phi)$ and maintaining the mainbeam amplitude in the direction (θ_0, ϕ_0) constant. Denote the perturbed patterns by $f_\theta(\theta, \phi)$ and $f_\phi(\theta, \phi)$ and the perturbed pattern element weights by w_{qi}, $i = 1, 2, \ldots N$; so that

$$f_\theta(\theta, \phi) = \sum_{i=1}^{N} w_{qli}\, e_{\theta i}(\theta, \phi) \tag{23a}$$

$$f_\phi(\theta, \phi) = \sum_{i=1}^{N} w_{qli}\, e_{\phi i}(\theta, \phi)\,. \tag{23b}$$

The $\{w_{qli}\}$ are then determined uniquely by the conditions that

$$f_\theta(\theta_0, \phi_0) = \sum_{i=1}^{N} w_{qli}\, e_{\theta i}(\theta_0, \phi_0) = f_{0\theta}(\theta_0, \phi_0)$$

$$= \sum_{i=1}^{N} w_{0i}\, e_{\theta i}(\theta_0, \phi_0) \tag{24a}$$

$$f_\phi(\theta_0, \phi_0) = \sum_{i=1}^{N} w_{qli}\, e_{\phi i}(\theta_0, \phi_0) = f_{0\phi}(\theta_0, \phi_0)$$

$$= \sum_{i=1}^{N} w_{0i}\, e_{\phi i}(\theta_0, \phi_0) \tag{24b}$$

(mainbeam constraints)

$$f_\theta(\theta_k, \phi_k) = \sum_{i=1}^{N} w_{qli}\, e_{\theta i}(\theta_k, \phi_k) = 0, \qquad k = 1, 2, \ldots, K \tag{25a}$$

$$f_\phi(\theta_k, \phi_k) = \sum_{i=1}^{N} w_{qli}\, e_{\phi i}(\theta_k, \phi_k) = 0, \qquad k = 1, 2, \ldots, K \tag{25b}$$

(null constraints)

and

$$|w_{q1i} - w_{0i}|^2 = \text{minimum} . \tag{26}$$

This system of equations can be put in an alternative equivalent form by letting

$$u_i = w_{qi} - w_{0i}, \qquad i = 1, 2, ..., N: \tag{27}$$

$$\sum_{i=1}^{N} u_i e_{\theta i}(\theta_0, \phi_0) = 0 \tag{28a}$$

$$\sum_{i=1}^{N} u_i e_{\phi i}(\theta_0, \phi_0) = 0 \tag{28b}$$

$$\sum_{i=1}^{N} u_i e_{\theta i}(\theta_k, \phi_k) = -f_{0\theta}(\theta_k, \phi_k), \qquad k = 1, 2, ..., K \tag{29a}$$

$$\sum_{i=1}^{N} u_i e_{\phi i}(\theta_k, \phi_k) = -f_{0\phi}(\theta_k, \phi_k), \qquad k = 1, 2, ..., K \tag{29b}$$

$$\sum_{i=1}^{N} |u_i|^2 = \text{minimum} . \tag{30}$$

In matrix form, Eqs. (28) and (29) can be written as

$$C^{\dagger} \underline{u} = \underline{g}_1 \tag{31}$$

where

$$C^{\dagger} = \begin{bmatrix} e_{\theta 1}(\theta_0, \phi_0) & e_{\theta 2}(\theta_0, \phi_0) \cdots e_{\theta N}(\theta_0, \phi_0) \\ e_{\theta 1}(\theta_1, \phi_1) & e_{\theta 2}(\theta_1, \phi_1) \cdots e_{\theta N}(\theta_1, \phi_1) \\ \vdots & \vdots & \vdots \\ e_{\theta 1}(\theta_K, \phi_K) & e_{\theta 2}(\theta_K, \phi_K) \cdots e_{\theta N}(\theta_K, \phi_K) \\ e_{\phi 1}(\theta_0, \phi_0) & e_{\phi 2}(\theta_0, \phi_0) \cdots e_{\phi N}(\theta_0, \phi_0) \\ e_{\phi 1}(\theta_1, \phi_1) & e_{\phi 2}(\theta_1, \phi_1) \cdots e_{\phi N}(\theta_1, \phi_1) \\ \vdots & \vdots & \vdots \\ e_{\phi 1}(\theta_K, \phi_K) & e_{\phi 2}(\theta_K, \phi_K) \cdots e_{\phi N}(\theta_K, \phi_K) \end{bmatrix} \tag{32}$$

and

$$\underline{g}_1 = \begin{bmatrix} 0 \\ -f_{0\theta}(\theta_1, \phi_1) \\ \vdots \\ -f_{0\theta}(\theta_K, \phi_K) \\ 0 \\ -f_{0\phi}(\theta_1, \phi_1) \\ \vdots \\ -f_{0\phi}(\theta_K, \phi_K) \end{bmatrix}. \tag{33}$$

$C^\dagger$ has dimensions M x N and $\underline{g}_1$ dimension M where M, the number of constraints, is equal to 2 (K + 1) where K is the number of null directions. The solution to Eq. (31) that minimizes $|\underline{u}|^2$ is[36]

$$\underline{u} = C\,(C^\dagger C)^{-1}\,\underline{g}_1 \tag{34}$$

which, with Eq. (25), yields the quiescent weight vector $\underline{w}_{q1}$.

$$\underline{w}_{q1} = \underline{u} + \underline{w}_0. \tag{35}$$

The vector $\underline{w}_q$ needed in Eq. (5) is obtained from the solution of

$$C^\dagger \underline{w}_q = \underline{g}, \tag{36}$$

$$\underline{g} = \begin{bmatrix} f_{o\theta}(\theta_0, \phi_0) \\ 0 \\ \vdots \\ f_{o\phi}(\theta_0, \phi_0) \\ 0 \\ \vdots \\ 0 \end{bmatrix} \tag{37}$$

that minimizes $|\underline{w}_q|^2$, namely [cf. Eq. (2b)]

$$\underline{w}_q = C\,(C^\dagger C)^{-1}\,\underline{g}. \tag{38}$$

With C, $\underline{w}_{q1}$, and $\underline{w}_q$ known, it remains to obtain the blocking matrix W_B. As mentioned in Section 2, W_B is not unique, and many different algorithms can be used leading to different W_B's. Here we use a variant of a method due to Trudnowski[37] that is easily implemented. The

---

[36] Rao, C.R., and Mitra, S.K. (1971) *Generalized Inverse of Matrices and Its Applications*, John Wiley, New York, Chap. 3.

[37] Trudnowski, D.J. (1988) *Adaptive Array Beamforming Using the Generalized Sidelobe Canceller*, Electronic Research Laboratory, Rept. No. 188, Montana State University, Bozeman, MT 59717.

method calculates the elements of the N – (M + 1) columns of W_B, column by column. To obtain the elements of the jth column of W_B we first set all N elements of the jth column equal to zero except for M + 2 consecutive elements starting with the jth element. This choice of nonzero elements assures that the columns of W_B are linearly independent as required. The jth element of the column is set equal to unity and the next M + 1 elements are unknowns to be determined by satisfying the orthogonality condition, Eq. (4). Multiplying the M + 1 rows of $[C|\underline{w}_1]^\dagger$ in turn by the jth column of W_B and equating the products to zero we obtain

$$\sum_{n=1}^{N} C^{\dagger}_{mn} W_{Bnj} = C^{\dagger}_{mj} + \sum_{n=j+1}^{j+(M+1)} C^{\dagger}_{mn} W_{Bnj} = 0, \qquad m = 1, 2, \ldots, M \tag{39a}$$

$$\sum_{n=1}^{N} w^{*}_{1n} W_{Bnj} = w^{*}_{1j} + \sum_{n=j+1}^{j+(M+1)} w^{*}_{1n} W_{Bnj} = 0. \tag{39b}$$

This is a set of M + 1 linear equations that can be solved for the M + 1 unknowns of the jth column of W_B provided that the equation system is nonsingular. It should be noted that the equation system [Eq. (37)] can be singular, in which case a different choice of the M + 1 unknown elements of the jth column of W_B must be made. Since the rank of $[C|\underline{w}_1]^\dagger$ is M + 1, we are assured that some choice of the M + 1 unknown elements of the jth column of W_B will result in a nonsingular equation system.

Having discussed the general computation procedure for implementing the GSC for arrays, we proceed in the next section to discuss how the computations are performed for a particular hybrid antenna configuration – an offset parabolic reflector with a focal plane feed array.

4. OFFSET PARABOLOIDAL REFLECTOR

In this and the following section, to illustrate the general formalism we have presented in Sections 2 and 3, we discuss the example of an array-fed offset paraboloidal reflector (see Figure 2). The reflector is a section of the paraboloid with focal length F given by the equation

$$z = (x^2 + y^2)/4F - F \tag{40}$$

in the cartesian coordinate system centered at the focus and with the z-axis as the paraboloid axis. The reflector is assumed to be symmetric about the xz-plane, and to have a circular projection in the xy-plane with diameter D. The center of the circular projection is offset a distance d_0 from the z-axis.

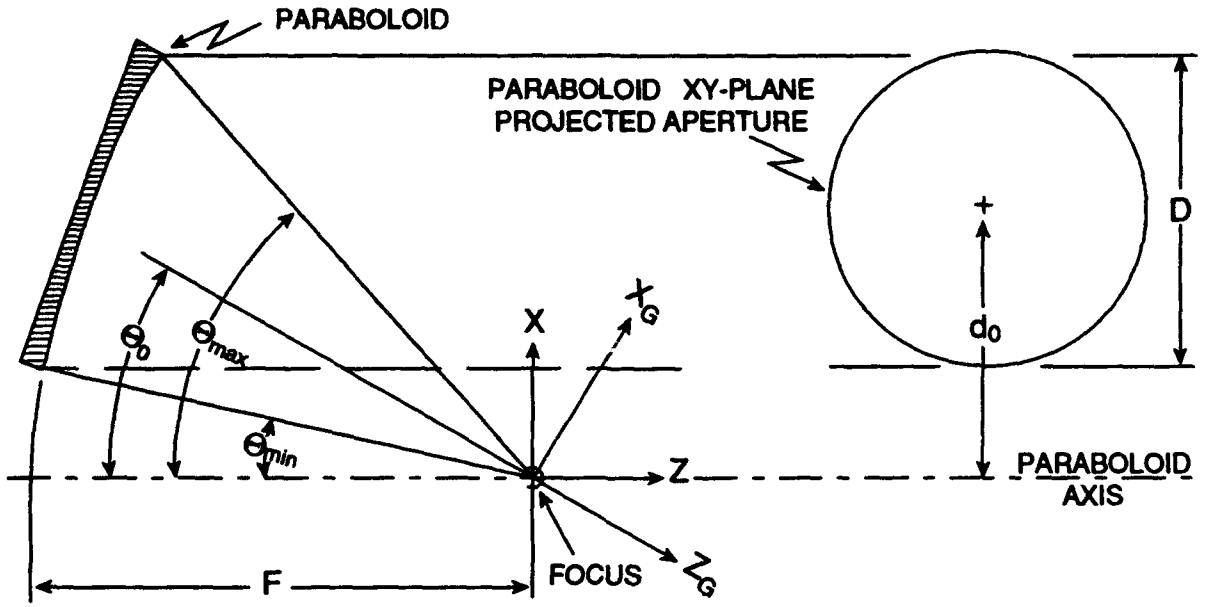

Figure 2. Offset Parabolic Reflector Geometry

The elements of the array feed are assumed to be located in the plane through the focus normal to the ray from the focus to the center of the circle formed by the reflector rim as seen from the focus. This ray makes an angle of θ_0 obtainable from the relations [38]

$$\theta_{max} = 2 \tan^{-1} [(d_0 + D/2)/2F] \quad (41a)$$

$$\theta_{min} = 2 \tan^{-1} [(d_0 - D/2)/2F] \quad (41b)$$

$$\theta_0 = (\theta_{max} + \theta_{min})/2. \quad (41c)$$

---

[38] Rahmat-Samii, Y. (1988) Reflector antennas, *Antenna Handbook*, Y.T. Lo and S.W. Lee, Eds., Van Nostrand Reinhold, New York, Chap. 15.

The location of the elements of the array feed is conveniently given in terms of an auxiliary cartesian coordinate system, (x_G, y_G, z_G), as shown in Figure 2, with origin at the focus and

$$x_G = x \cos\theta_0 + z \sin\theta_0 \tag{42a}$$

$$y_G = y \tag{42b}$$

$$z_G = 0 = -x \sin\theta_0 + z \cos\theta_0. \tag{42c}$$

All array elements are assumed to be ideal dipoles electrically polarized in the x_G-direction and to radiate a spherical wave given by[38]

$$\underline{E}(r_F) = A_0 \exp\left[\left(-j2\pi r_F\right)/\lambda\right]/r_F\left(\cos\theta_F \cos\phi_F\, \hat{\theta}_F - \sin\phi_F\, \hat{\phi}_F\right), \qquad 0 \le \theta_F \le \pi/2 \tag{43}$$

$$= 0, \qquad \theta_F > \pi/2$$

where $\underline{E}$ is the electric field at the field point with spherical coordinates (r_F, θ_F, ϕ_F) referred to a cartesian coordinate system with origin at the element, z_F-axis in the opposite direction to the z_G-axis (normal to the array plane), x_F-axis parallel to the x_G-axis, and y_F-axis in the opposite direction to the y-axis. A_0 is the complex excitation coefficient of the feed element.

In programming the GSC implementation of adaptive nulling with an array-fed offset paraboloidal reflector antenna, we have made extensive use of the work of Rusch and Prata[25,26] who developed computer programs to calculate the focal-region fields of offset single and dual reflectors, and to calculate the radiation fields of array-fed offset single and dual reflector antennas. We have programmed only the steady-state (non-time-varying) implementation of the GSC. The major steps of the implementation of the GSC are as follows:

1) Obtain a starting set of array element weights $\{w_{0i}\}$ (see Section 3) that give an antenna pattern with low sidelobes and mainbeam directed in a specified direction.

This is accomplished by assuming a tapered plane wave incident on the paraboloid aperture[25] from the direction that the mainbeam is to point, and calculating the field at the array element locations by physical optics (PO) integration over the paraboloid surface, using Rusch and Prata's computer program OFRADC.[25] The $\{w_{0l}\}$ are then taken to be the complex conjugates of the x_G-component of the electric field at the elements.

2) Calculate the modified set of weights $\{w_{ql}\}$ that will yield an antenna pattern with nulls at specified directions and that will otherwise be as close as possible to the original (design) pattern keeping the mainbeam amplitude constant.

This is accomplished by first calculating the elements of the constraint matrix [Eq. (32)], the outputs of the individual feed elements on receive in response to unit amplitude θ- and ϕ-electrically polarized plane waves incident on the reflector from the mainbeam and desired null directions. (We ignore here any direct illumination of the feed elements by the incoming plane waves.) By reciprocity, they are also given as the θ- and ϕ-components of the electric far field in the mainbeam and null directions resulting from unit excitation of the individual feed elements, and are calculated using a modified version of Rusch and Prata's computer program OFPARA.[25] Also calculated are the elements of the vectors $\underline{g}_1$ [Eq. (33)] and $\underline{g}$ [Eq. (37)] which involve the values of the unmodified antenna pattern in the mainbeam and null directions. The modified quiescent weight vector $\underline{w}_{ql}$ is then obtained from Eqs. (34) and (35), and the weight vector $\underline{w}_q$ from Eq. (38).

3) Calculate the elements of the array data covariance matrix $R_{\underline{z}\underline{z}}$ assuming an environment of uncorrelated signal and interferer sources specified by direction, amplitude, and polarization. Signal and interference strength are referred to the 0 dB level assumed for the internal noise of each array feed element.

By reciprocity this is accomplished by using Rusch and Prata's program OFPARA, modified to calculate the sum of the θ- and ϕ-components of the electric far field radiated by each feed element in each source direction, appropriately weighted by the magnitudes and polarizations of the sources. The covariance matrix is then formed by summing the products of the complex conjugate and transpose of the vectors of fields radiated by the feed elements in each of the source directions, and adding the value of unity to the diagonal elements of the resulting matrix to represent the internal noise.

4) Calculate the blocking matrix W_B by the algorithm described in Section 3 and finally the adapted weight vector $\underline{w}_a$ from Eq. (13) and the set of effective weights $\underline{w}$ for the GSC from Eq. (14). Alternatively calculate $\underline{w}$ from Eq. (19).

For any given set of array weights, the corresponding antenna pattern was calculated using Rusch and Prata's program OFPARA. Co- and cross-polar fields were calculated using Ludwig's third definition.[39] All calculations were performed in double precision on a VAX 8650 computer.

5. CALCULATIONS

This section shows the results of the calculations performed to illustrate the theory. In all calculations the values of the diameter D, the focal length F, and the offset distance d_0 of the paraboloid, were taken to be 100λ, 100λ, and 60λ, respectively. A square feed array of 81 elements (9 x 9), centered on the focus, with 0.75λ spacing was used. The mainbeam direction was taken to be $\phi = 90°$, $\theta = 1.0°$ (scanned one degree off axis). Unless otherwise noted the source environment consists of a –20 dB signal in the mainbeam direction, electrically polarized in the ϕ-direction, and 40 dB ϕ-polarized interference at $\phi = 90°$, $\theta = 3.4°$. Internal white noise at a 0 dB level is assumed present for each element of the feed.

Figure 3 shows the H-plane ($\phi = 90°$ or yz-plane) design patterns. Here, as in all the plots, solid and dashed curves are used to indicate the co- and cross-polar patterns, respectively. The first sidelobes of the co-polar pattern, located at $\theta = -0.83°$ and 2.3°, are -35 and -29 dB down from the mainbeam peak, respectively.

In Section 2 the important point was made that appending the $\underline{w}_1$-vector (see discussion on pg. 7, following Eq. (5)), to the constraint matrix containing the mainbeam and null constraints, is essential if the quiescent pattern (the quiescent pattern is the pattern obtained when the GSC operates in the presence of uncorrelated data, or equivalently, when the covariance matrix of the array data vector $R_{\underline{x}\underline{x}}$, Eq. (9), is equal to the identity matrix) is equal to the initial, unadapted pattern (the pattern corresponding to the weight vector $\underline{w}_{q1}$ in the upper path of the GSC). (We will refer to the $\underline{w}_1$-vector appended to the constraint matrix as "the pattern constraint".) Illustrating this point, Figure 4 shows the H-plane quiescent patterns obtained given white noise input, when the $\underline{w}_1$-vector is not appended. In this example the constraint matrix contains only the mainbeam constraints. The patterns shown in Figure 4 correspond to the weight vector $\underline{w}_q$ of Eq. (2b) even though the weight vector $\underline{w}_{q1}$ of Eq. (2a) is placed in the upper path of the GSC. It is apparent from comparing Figure 4 with Figure 3 how important the pattern constraint is. The first sidelobes of the H-plane co-polar quiescent pattern, move in to 0.0° and 2.0°, with the sidelobe at 0.0° now only -16 dB below the mainbeam. If the pattern constraint is employed, then the quiescent patterns are, of course, identical with those of Figure 3.

---

[39] Ludwig, A.C. (1973) The definition of cross polarization, *IEEE Trans. Antennas Propagat.*, **AP-21**:116-119.

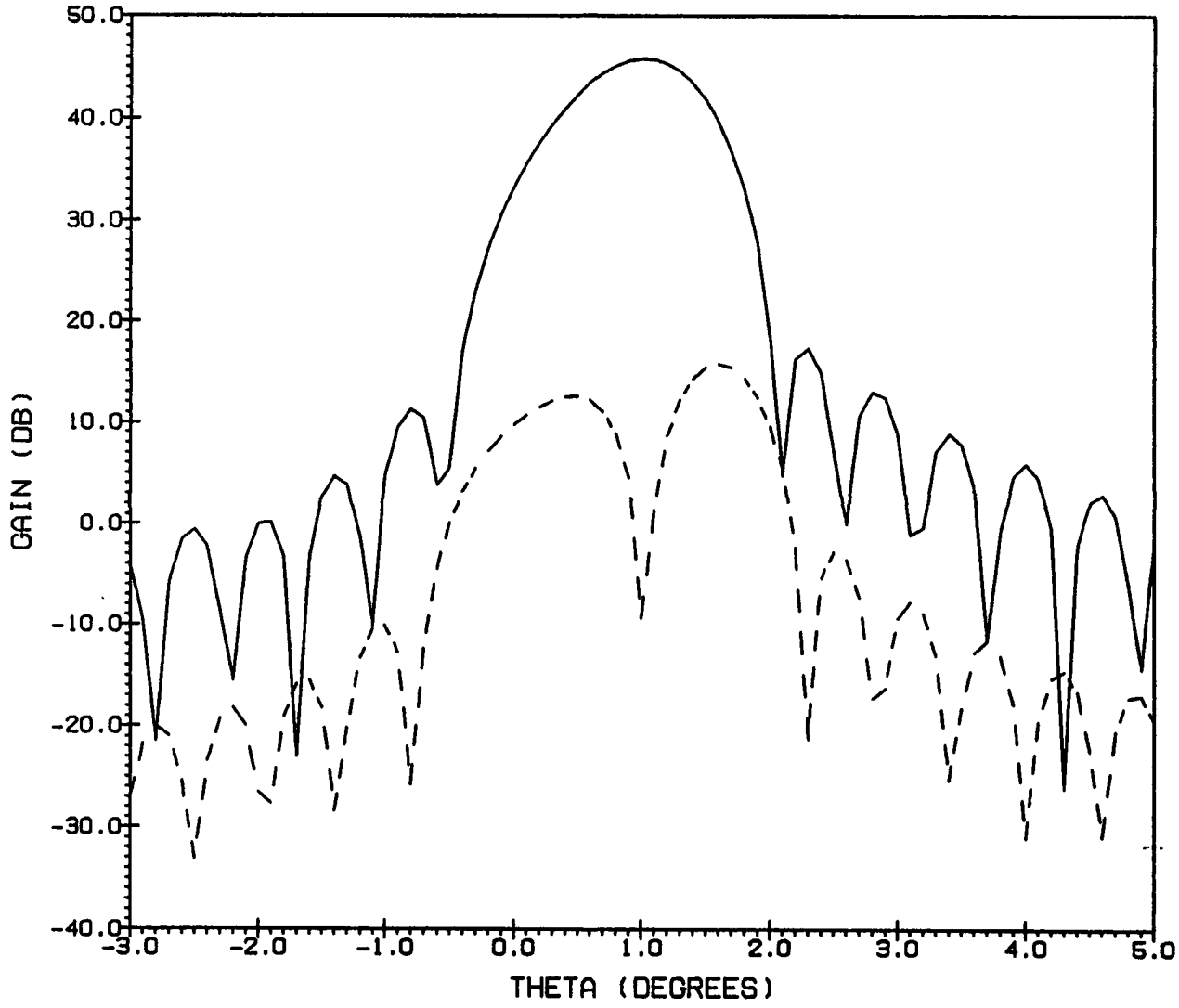

Figure 3. H-Plane Design Patterns; _____ Co-polar, ----- Cross-polar.

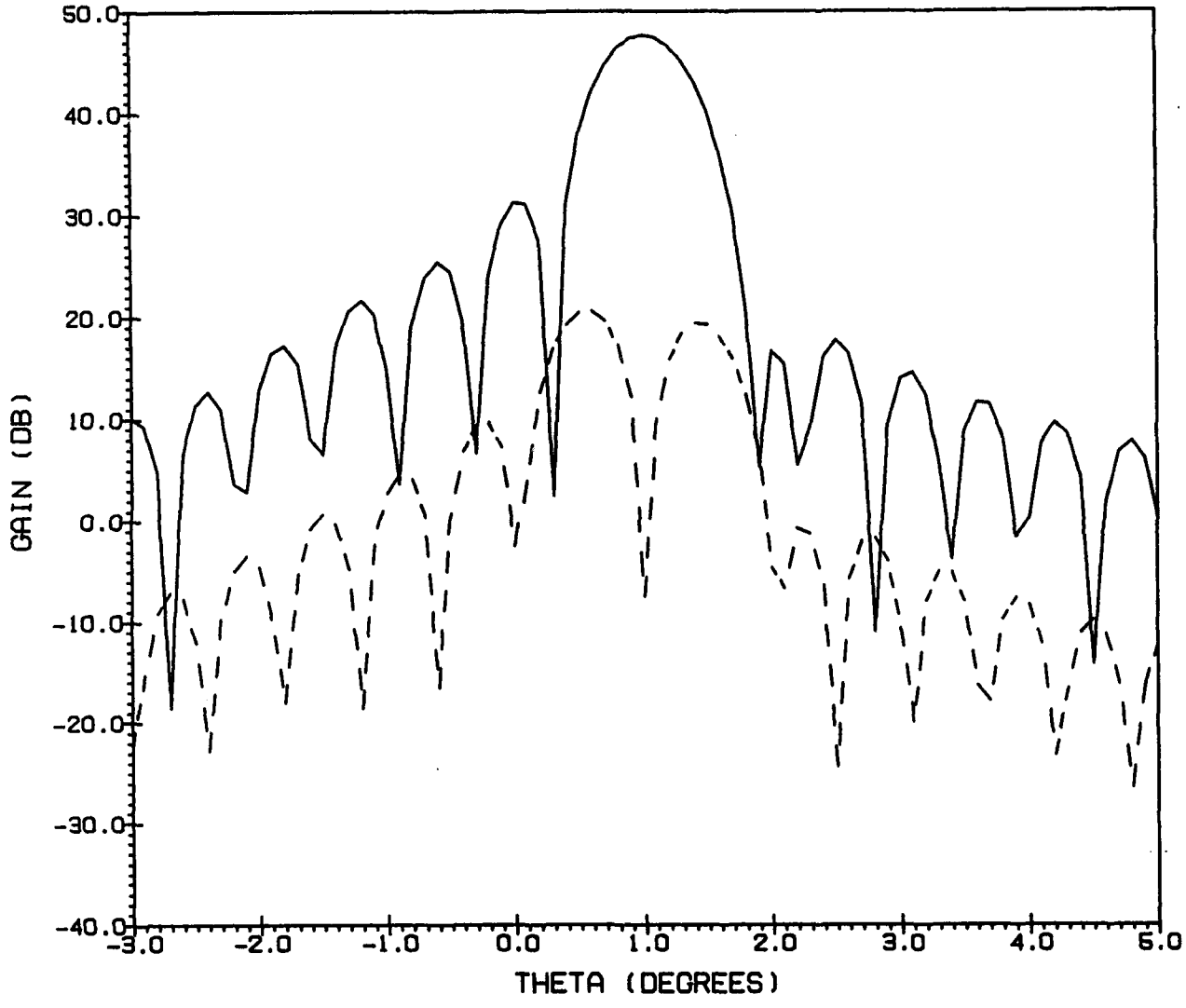

Figure 4. H-Plane Quiescent Patterns, No Pattern Constraint; _____Co-polar,----- Cross-polar.

Figure 5 shows the H-plane adapted patterns when both the pattern and mainbeam constraints are employed. A deep null has been formed in the co-polar pattern at $\theta = 3.4^\circ$ corresponding to the location and polarization of the interference. The adapted patterns to the left of the first sidelobe at $\theta = 2.4^\circ$ bear a reasonably close resemblance to the design patterns of Figure 3, while the adapted patterns to the right of the first sidelobe are pulled down considerably compared to the design patterns of Figure 3.

In contrast, Figure 6 shows the H-plane adapted patterns when the pattern constraint has not been employed. Comparison of Figure 6 with the design patterns shown in figure 3 and the adapted patterns of Figure 5 obtained using the pattern constraint, shows how important the pattern constraint is if the adapted pattern is to have any resemblance to the unadapted pattern. Although the co-polar pattern in Figure 6 has a deep null at $\theta = 3.4^\circ$ as desired, the remainder of the co-polar pattern, and all of the cross-polar pattern, are in fact very close to the $\underline{w}_q$-patterns of Figure 4. This, of course, is not surprising since the adapted patterns of Figure 6 are exactly those that would have been obtained if the $\underline{w}_q$-weight vector of Eq. (2b) had been placed in the upper path of the GSC instead of the $\underline{w}_{q1}$-weight vector of Eq. (2a).

As an example of how the adapted patterns change with the polarization of the interference at $\phi = 90^\circ$, $\theta = 3.4^\circ$, Figure 7 shows the H-plane adapted patterns when the interference is electrically θ-polarized rather than ϕ-polarized as in Figure 5. Here the adapted null at $\theta = 3.4^\circ$ is placed in the cross-polar pattern rather than in the co-polar pattern. The remainder of the cross-polar pattern, and the entire co-polar adapted pattern, are seen to be very close to the design patterns of Figure 3. The reason why the adapted patterns of Figure 7 bear a considerably closer resemblance to the design patterns of Figure 3 than do the adapted patterns of Figure 5 probably lies in the fact that the cross-polar design pattern of Figure 3 aleady has a fairly deep null at $\theta = 3.4^\circ$ and so requires a relatively small change to adapt to the presence of the θ-polarized interference at 3.4°. In contrast, the co-polar design pattern at $\theta = 3.4^\circ$ is 34 dB higher than the cross-polar pattern and so requires a considerably larger change to adapt to the presence of the ϕ-polarized interference.

It is of interest to see what happens when the interference has both θ- and ϕ-components. Figure 8 shows the H-plane adapted patterns when the interference at $\theta = 3.4^\circ$ has equal θ- and ϕ-polarized components. Note that at $\theta = 3.4^\circ$, the co-polar and cross-polar patterns are equal at 66 dB below the mainbeam. Thus neither pattern has as deep a null as that formed when the interference has only one component. In other respects, the patterns are quite similar to those of Figure 5, the adapted patterns obtained when the intereference is ϕ-polarized only, especially the patterns to the left of $\theta = 3.0^\circ$. The reason why the null depths are deeper when the interference has only one polarization component is that the contributions of the θ- and ϕ-components of the interference to the array data vector are fully correlated with each other. The corresponding covariance matrix R_{zz} therefore contains cross products from the θ- and ϕ-components and hence results in a different set of adapted weights than would be obtained if the θ- and ϕ-components had to be cancelled separately. If, for example, there were two completely uncorrelated interferers in the direction $\theta = 3.4^\circ$, one θ-polarized and the other ϕ-polarized, both the co- and cross-polar adapted patterns would have null depths like those in Figures 5 and 7.

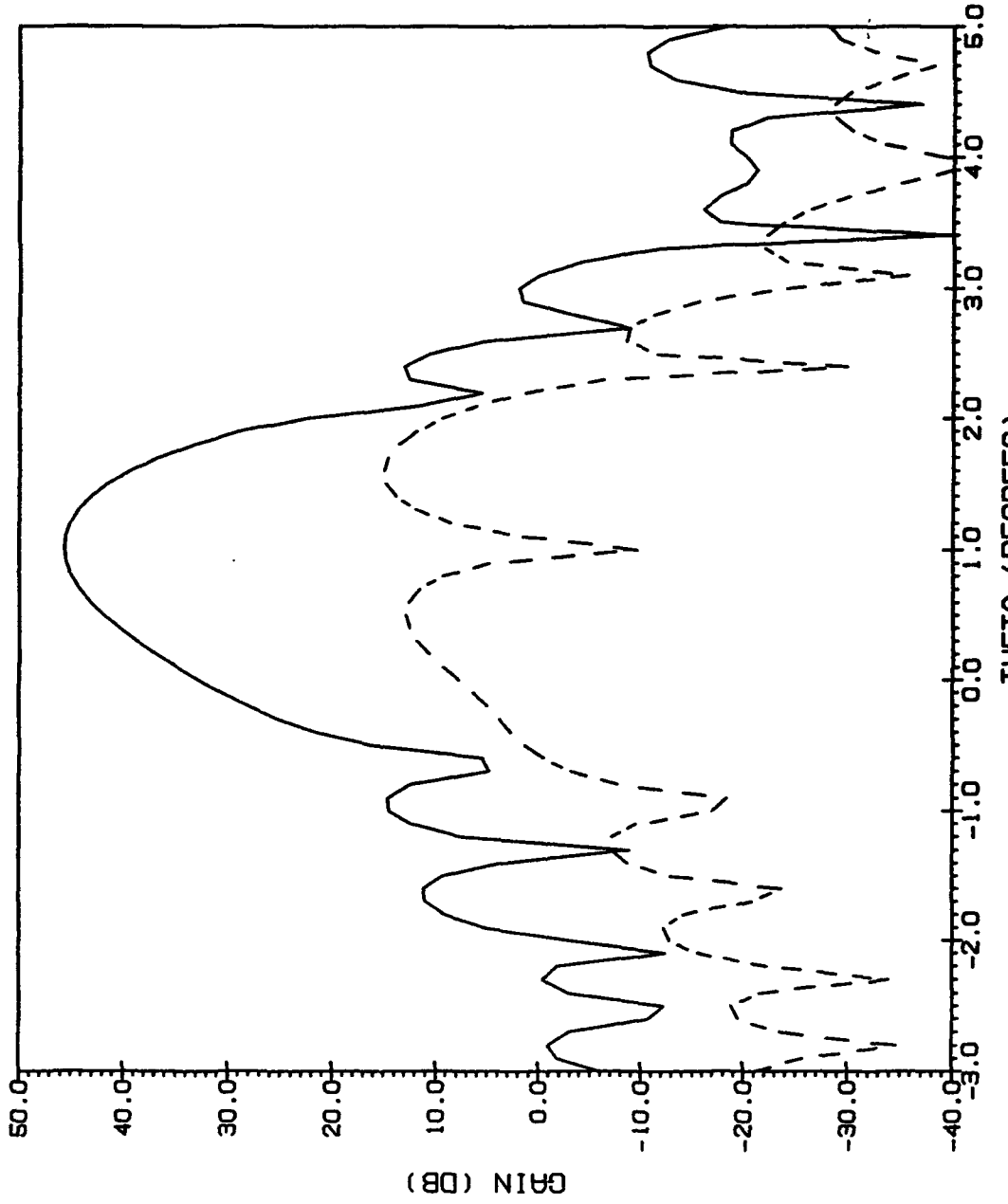

Figure 5. H-Plane Adapted Patterns, ϕ-Polarized Interference at $\phi = 90°$, $\theta = 3.4°$; ___ *Co-polar,* ----- *Cross-polar.*

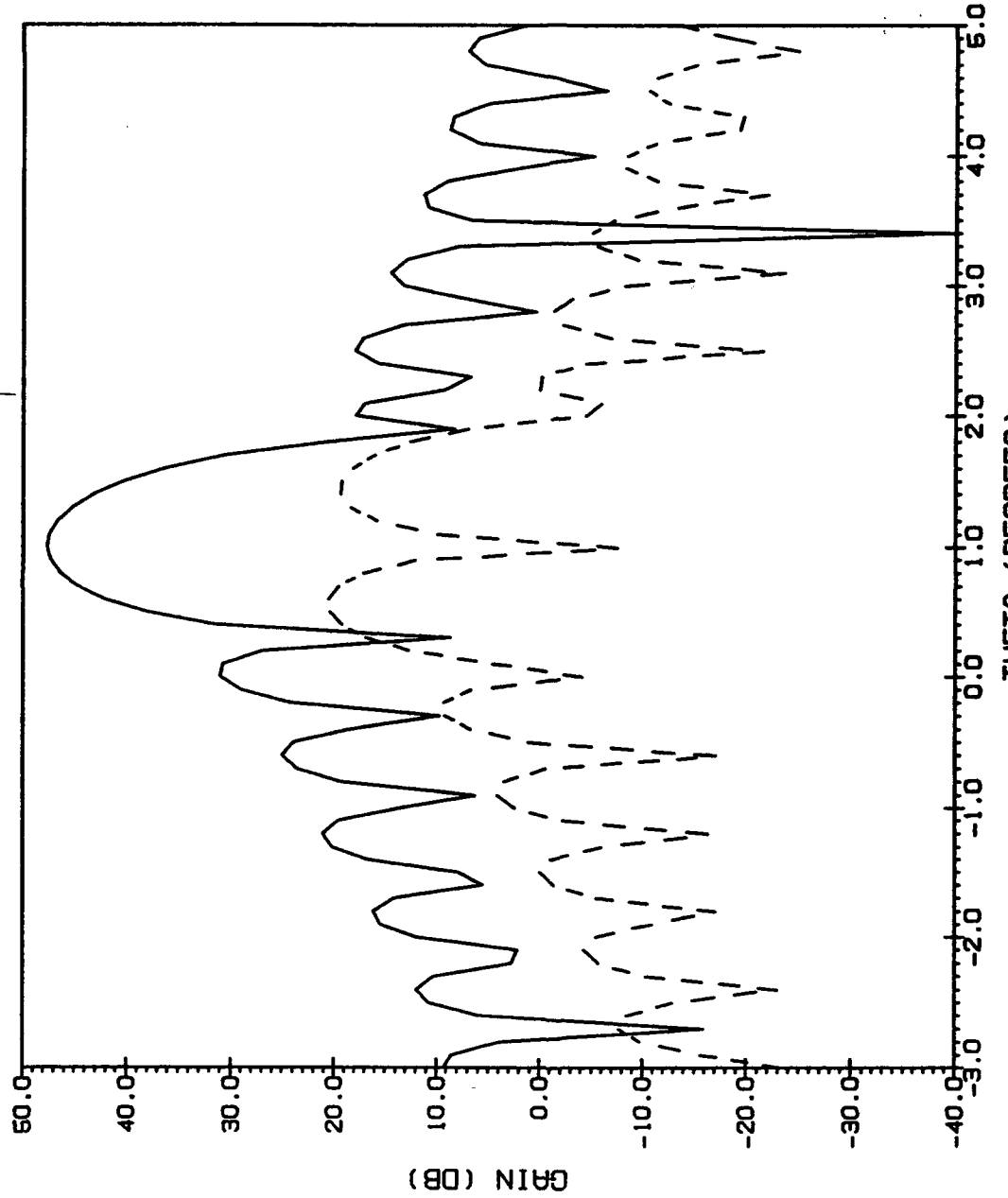

Figure 6. H-Plane Adapted Patterns, ϕ-Polarized Interference at $\phi = 90°$, $\theta = 3.4°$; No Pattern Constraint; _ Co-polar, ----- Cross-polar.

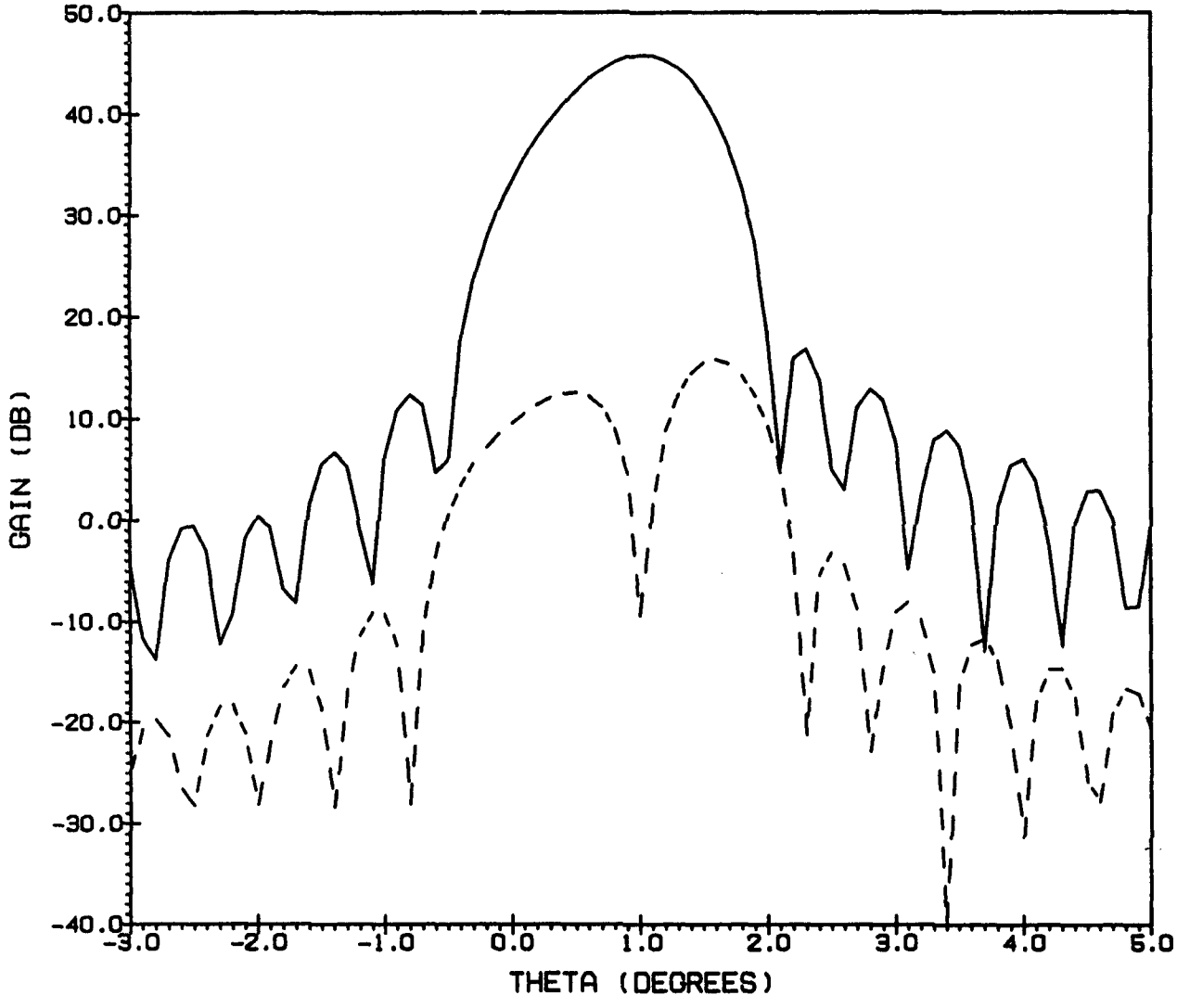

Figure 7. H-Plane Adapted Patterns, θ-Polarized Interference at $\phi = 90°$, $\theta = 3.4°$; ___ Co-polar, ----- Cross-polar.

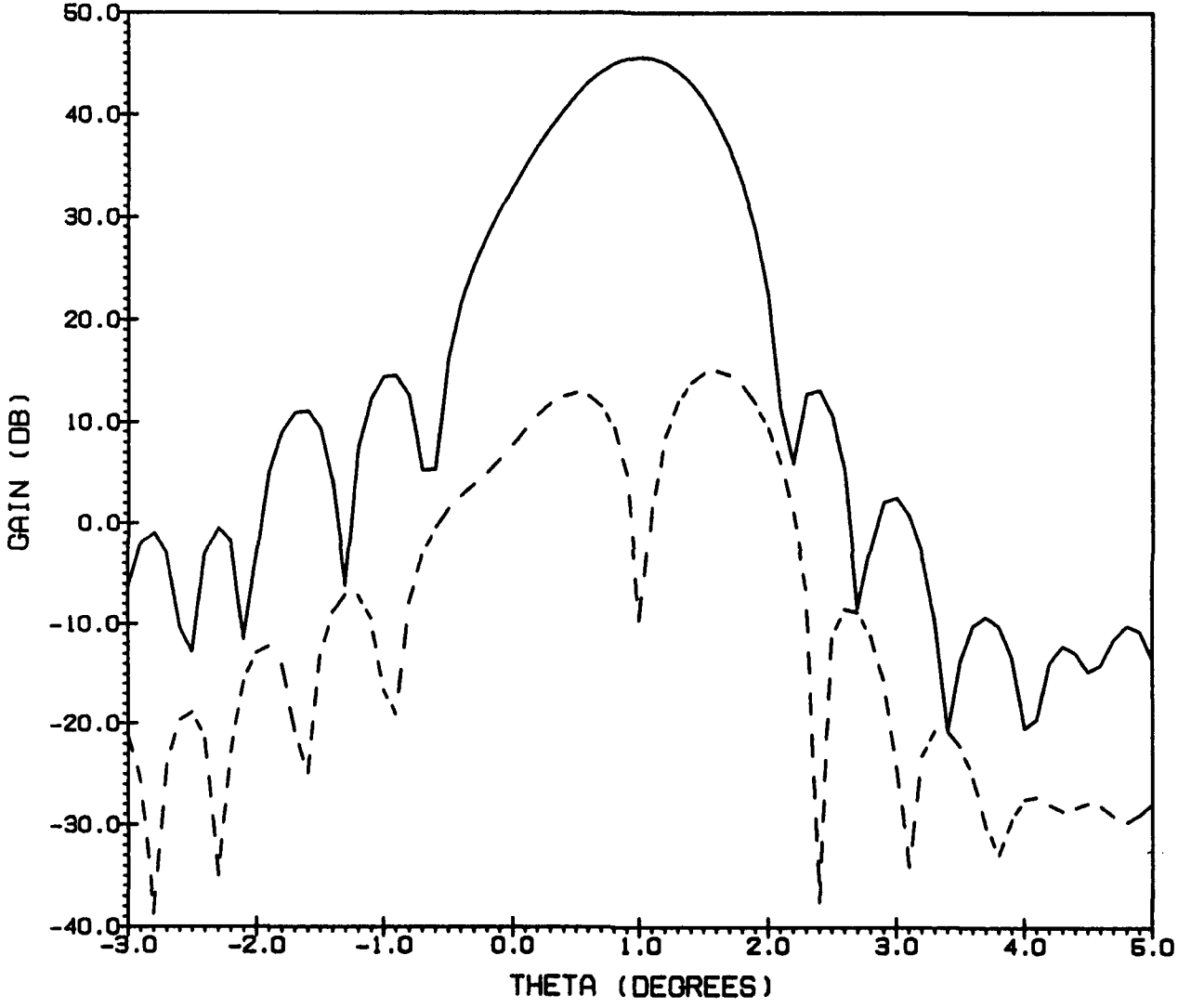

Figure 8. H-Plane Adapted Patterns, Interference at $\phi = 90^{\circ}$, $\theta = 3.4^{\circ}$, With Equal ϕ- and θ- Components; ____ Co-polar, ----- Cross-polar.

The fact that the patterns of Figure 8 do not have as deep nulls at the location of the interference as those of Figures 5 and 7 does not mean, of course, that the interference is less effectively cancelled out. It just means that the contributions of the two polarization components to the array data vector tend to cancel each other out to some extent, and so, in effect, less "work" has to be done by the adaptive weights to cancel the interference.

Figure 9 shows the H-plane unadapted patterns when two deterministic nulls, at $\phi = 90°$, $\theta = 3.0°$ and $4.0°$, have been imposed in both the co- and cross-polar design patterns of Figure 3, while otherwise attempting to keep the imposed null patterns as close as possible to the patterns of Figure 3, thus in effect forming a new pair of design patterns which have two imposed nulls. Comparing Figure 9 with Figure 3 we see that imposing the nulls significantly changes the patterns. The sidelobes to the right of the mainbeam are lowered, the sidelobes to the left of the mainbeam are raised, and the central portions of both the co- and cross-polar patterns are also altered somewhat.

Figure 10 shows the H-plane patterns obtained with white noise input starting with the weights for the design patterns of Figure 9 in the upper path of the GSC, and employing the mainbeam and null constraints but omitting the pattern constraint. These are the patterns corresponding to the $\underline{w}_q$-weights of Eq. (2b). (Figure 10 thus stands in the same relation to Figure 9 as Figure 4 does to Figure 3.) Most of the features of the design patterns of Figure 9 are changed greatly, especially to the left of $\theta = 3.0°$. The co-polar mainbeam, for example, narrows considerably, and the sidelobe to the left of the mainbeam increases considerably.

Figure 11 shows the H-plane adapted patterns obtained starting with the weights for the design patterns of Figure 9 in the upper path of the GSC, using null constraints so that the adapted patterns will continue to have nulls at $\phi = 90°$, $\theta = 3.0°$ and $4.0°$, and employing the pattern constraint so that the patterns obtained with white noise input, the quiescent patterns, are identical with those of Figure 9. The adaptive procedure results in an additional null in the co-polar pattern at $\theta = 3.4°$. In general, the adapted patterns of Figure 11 strongly resemble the design patterns of Figure 9.

Figure 12 shows the H-plane adapted patterns obtained starting with the design weights of Figure 9 in the upper path of the GSC, omitting the null constraints, but continuing to use a pattern constraint. (With white noise input, the patterns obtained are therefore identical to those of Figure 9.) In this case, the adapted co-polar pattern has an adapted null at $\theta = 3.4°$, but no longer has the constrained nulls at $\theta = 3.0°$ and $4.0°$ of the co-polar adapted pattern of Figure 11. In other respects, however, the adapted patterns of Figure 11 bear a closer resemblance to those of Figure 9 than do the adapted patterns of Figure 11. The reason why the patterns of Figure 12 more closely resemble the design patterns of Figure 9 than do those of Figure 11 obtained with null constraints, is that when no null constraints are used there is a greater number of degrees of freedom available for nulling the interference at $\theta = 3.4°$ and for matching the design (quiescent) pattern as closely as possible. Intuitively, it is as if the nulls at $\theta = 3.0°$ and $4.0°$ are traded off slightly for the adapted null at $\theta = 3.4°$. In the case of Figure 11, no such tradeoff is possible because the nulls at $\theta = 3.0°$ and $4.0°$ are constrained. Hence the adapted null pattern at $\theta = 3.4°$ must be formed at the expense of the remainder of the pattern.

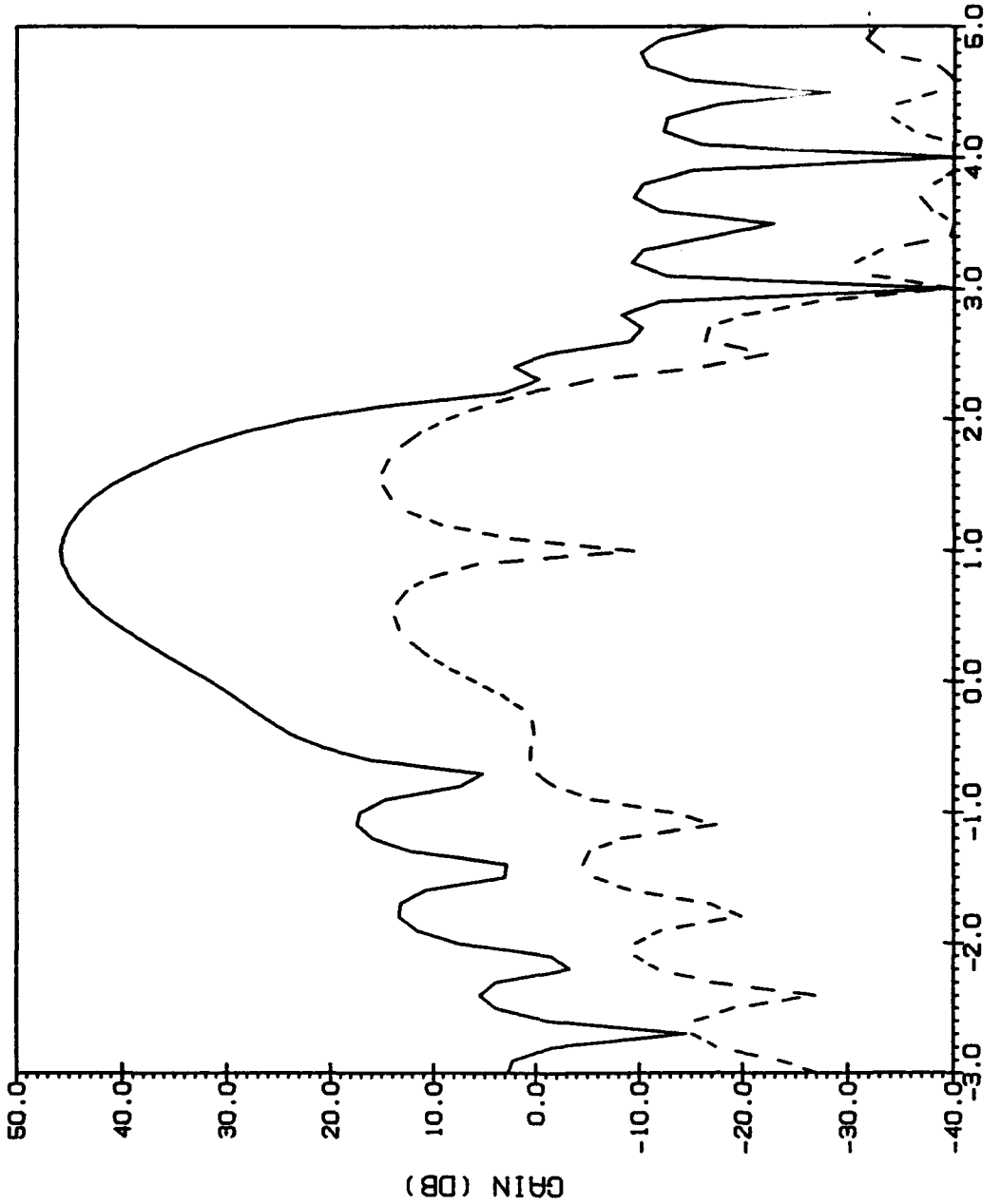

Figure 9. H-Plane Design Patterns With Nulls Imposed at $\phi = 90^{\circ}$, $\theta = 3.0^{\circ}$, 4.0°;
—— Co-polar, ----- Cross-polar.

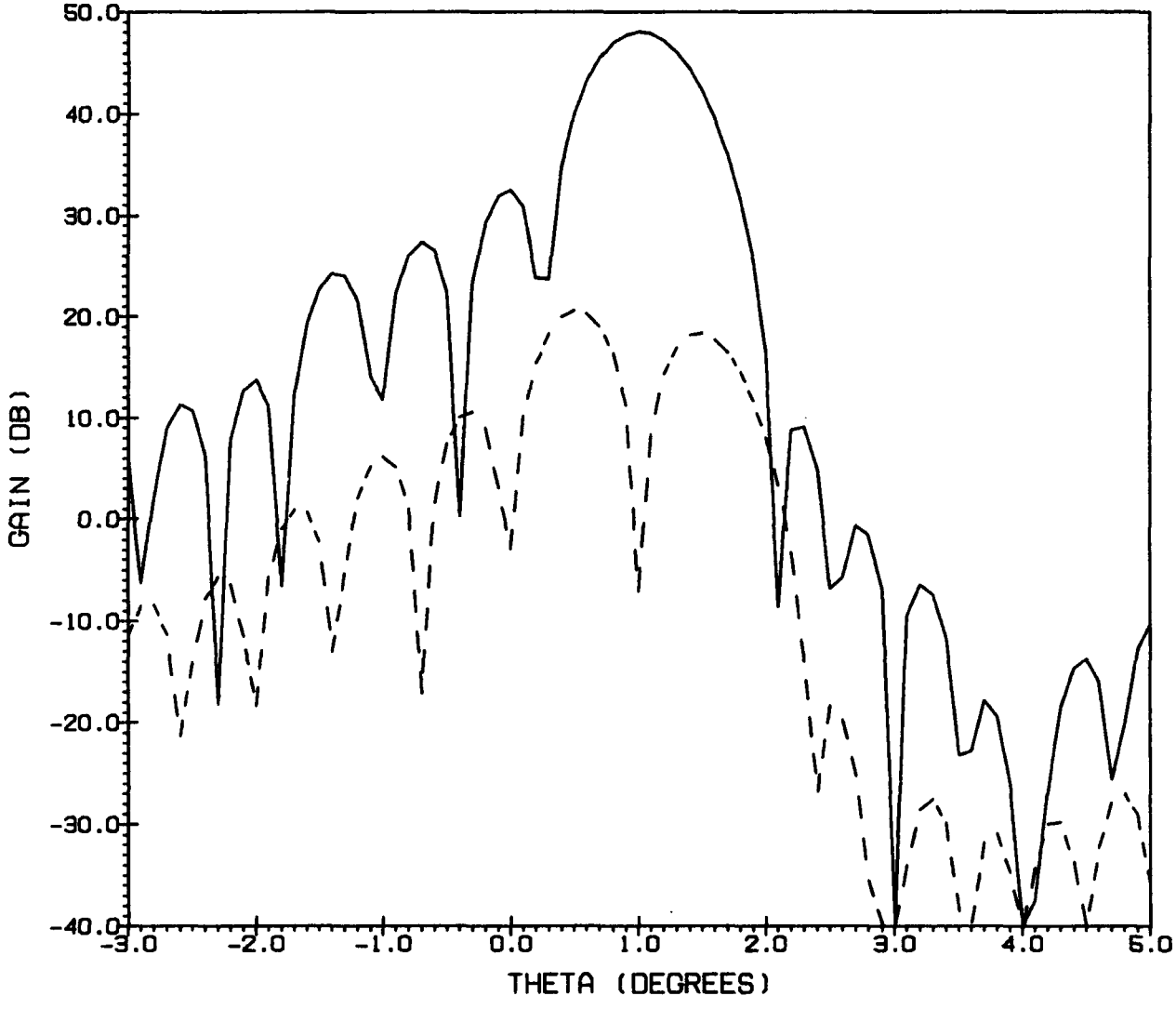

Figure 10. H-Plane Quiescent Patterns, No Pattern Constraint ; _____Co-polar, ----- Cross-polar.

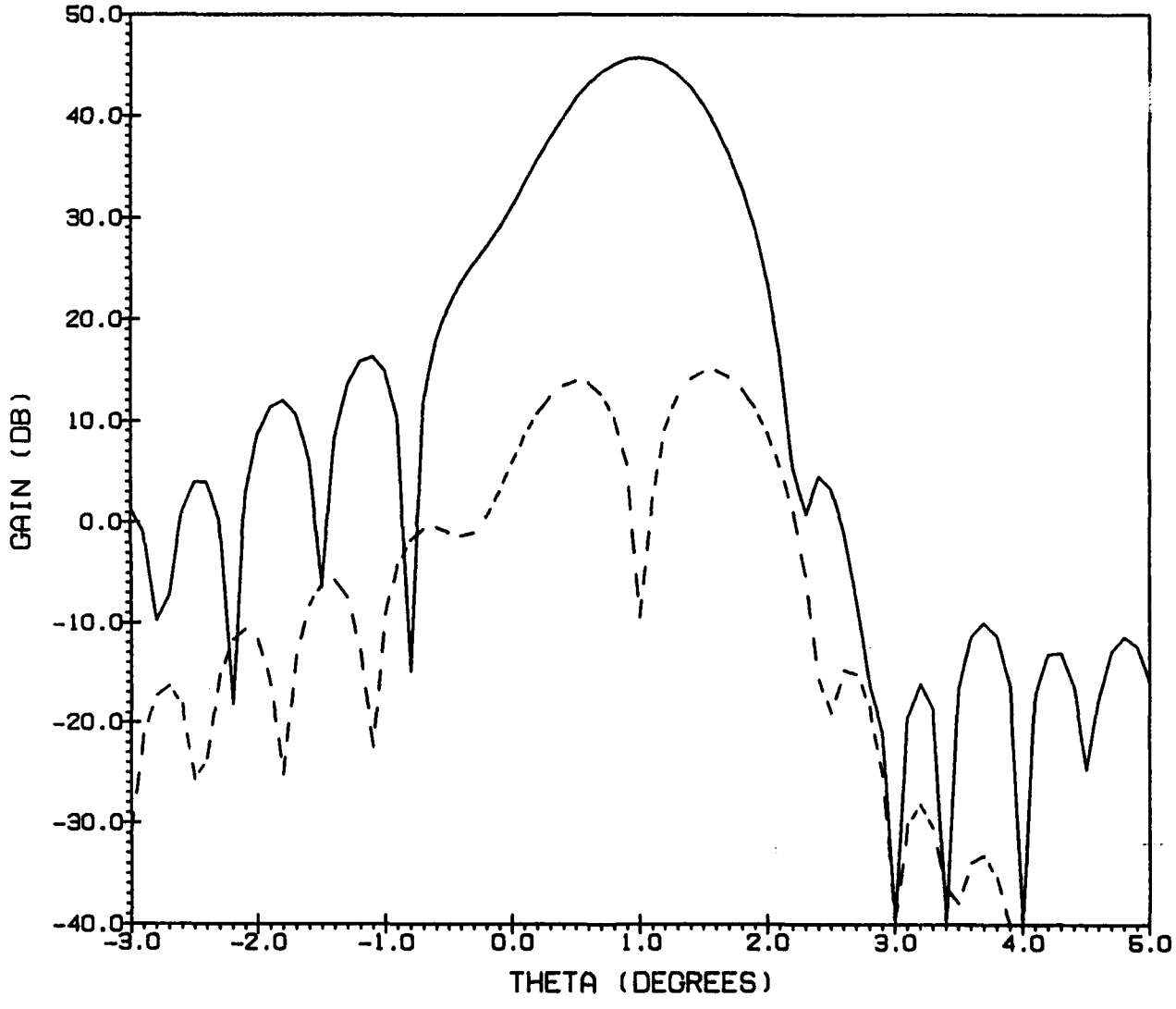

Figure 11. H-Plane Adapted Patterns, Pattern Constraint and Constrained Nulls at $\phi = 90^{o}$, $\theta = 3.0^{o}$, 4.0^{o}; ϕ-Polarized Interference at $\phi = 90^{o}$, $\theta = 3.4^{o}$; ____Co-polar, ----- Cross-polar.

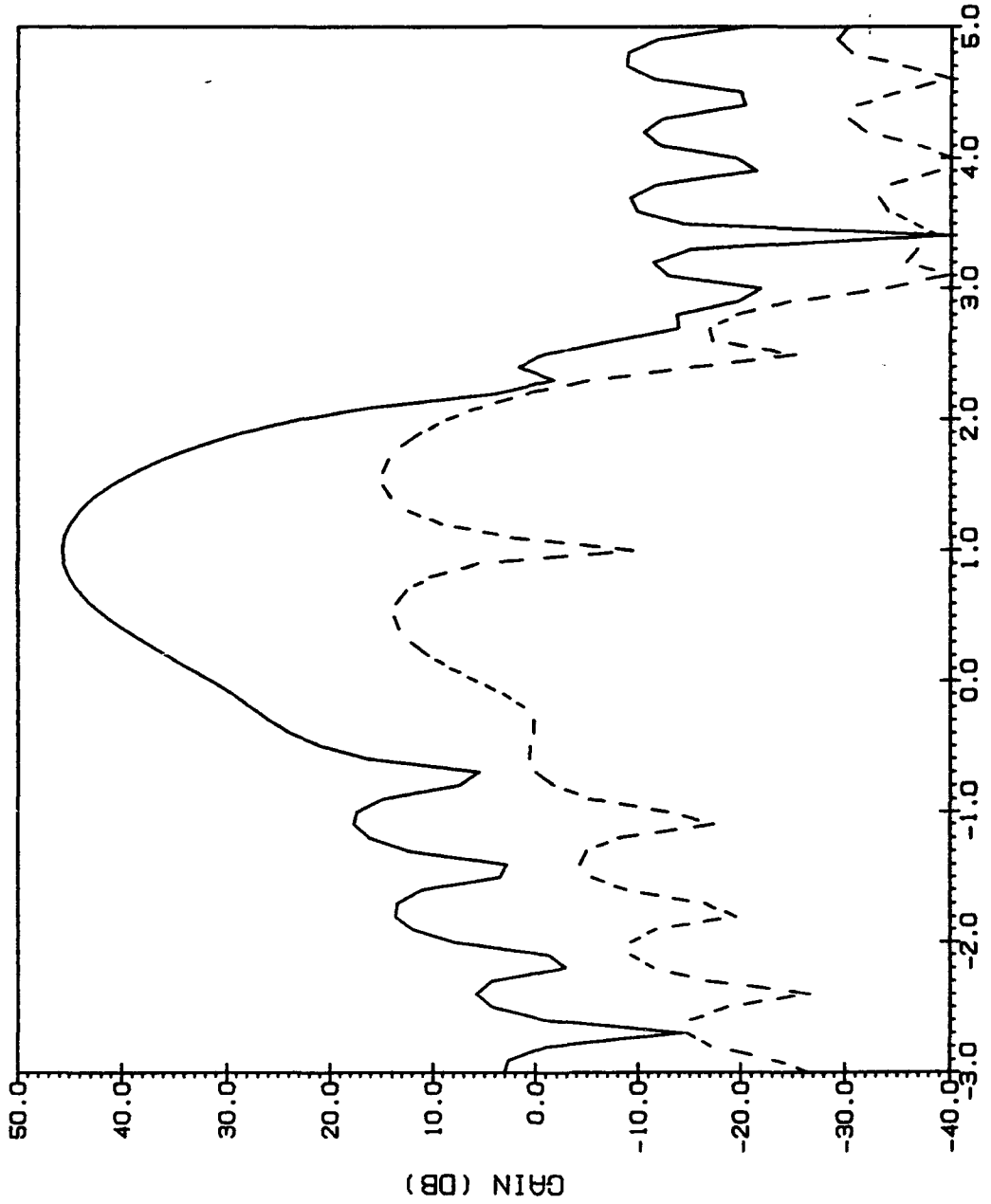

Figure 12. H-Plane Adapted Patterns, Pattern Constraint but No Constrained Nulls at $\phi = 90°, \theta = 3.0°, 4.0°$; ϕ-Polarized Interference at $\phi = 90°, \theta = 3.4°$, ____Co-polar, ----- Cross-polar.

Finally, Figure 13 shows the adapted H-plane patterns obtained starting with the design weights that correspond to Figure 9 in the upper path of the GSC, and employing the mainbeam and null constraints, *but not the pattern constraint*. To the left of $\theta = 3.0°$ the patterns obtained resemble very closely the patterns of Figure 10. This is not surprising since the components of the GSC are identical for the two figures, the difference being the presence of the interference at 3.4° which results in the adaptive null being placed at this location.

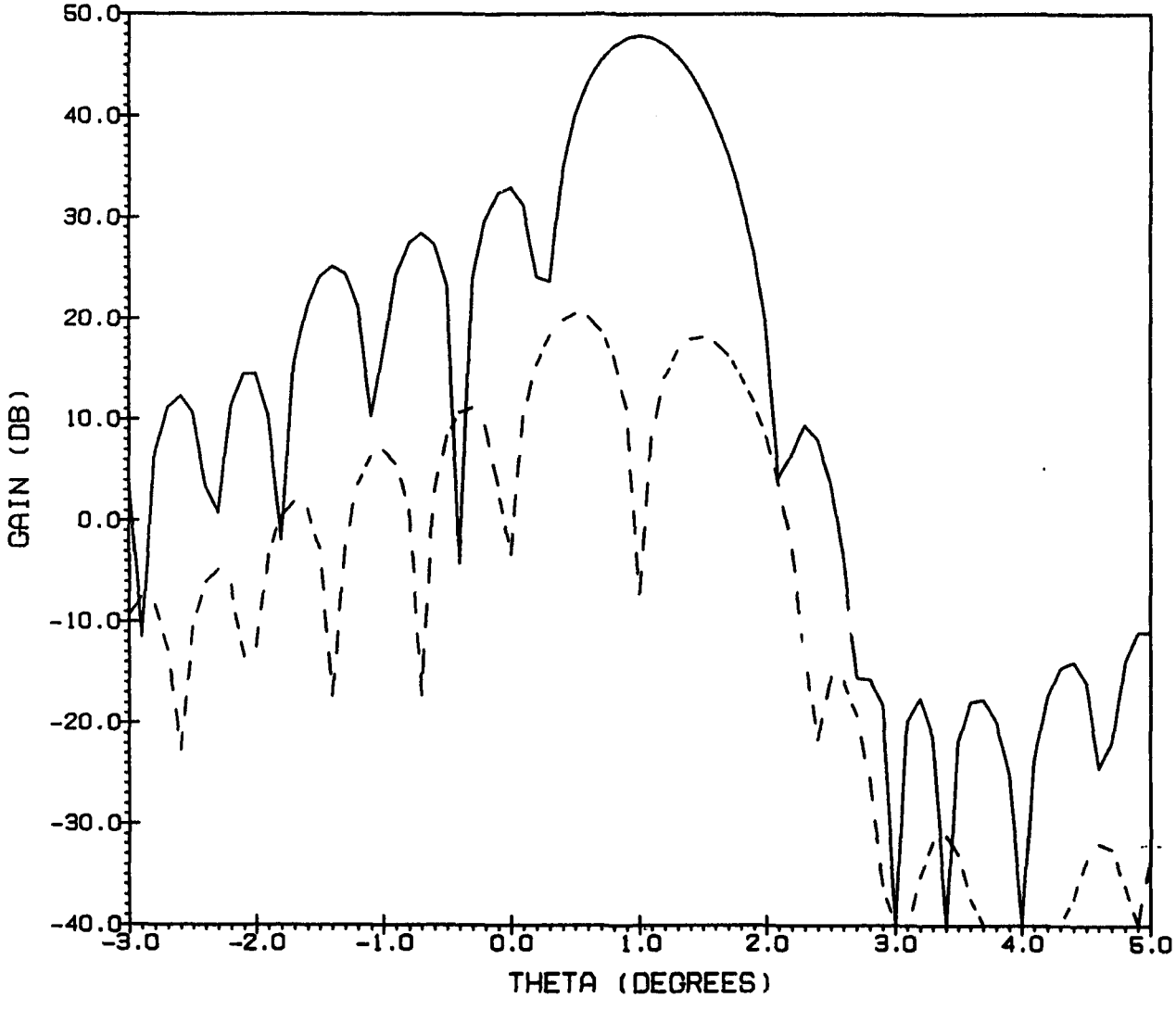

Figure 13. H-Plane Adapted Patterns, Constrained Nulls at $\phi = 90^{\circ}$, $\theta = 3.0^{\circ}$, 4.0°, No Pattern Constraint, ϕ-Polarized Interference at $\phi = 90^{\circ}$, $\theta = 3.4^{\circ}$; ____ Co-polar, ----- Cross-polar.

References

1. Mailloux, R.J. (1982) Hybrid antennas, *The Handbook of Antenna Design*, Vol. 1, A.W. Rudge et al, Eds., Peter Peregrinus, Ltd., London, Chap. 5.

2. Rudge, A.W., and Davies, D.E. (1970) Electronically controllable primary feed for profile-error compensation of large parabolic reflectors, *IEE Proc.*, **117**:351-358.

3. Blank, S.J., and Imbriale, W.A. (1988) Array feed synthesis for correction of reflector distortion and vernier beamsteering, *IEEE Trans. Antennas Propagat.*, **36**:1351-1358.

4. Cherrette, A.R., et al (1989) Compensation of reflector antenna surface distortion using an array feed, *IEEE Trans. Antennas and Propagat.*, **37**:966-978.

5. Rahmat-Samii, Y. (1990) Array feeds for reflector surface distortion compensation: concepts and implementation, *IEEE Antennas and Propagat. Magazine*, **32**:(No. 4)20-26.

6. Fante, R.L. (1980) Systems study of overlapped subarrayed scanning antennas, *IEEE Trans. Antennas Propagat.*, **AP-28**:668-679.

7. Mrstik, A.V., and Smith, P.G. (1981) Scanning capabilities of large parabolic cylinder reflector antennas with phased-array feeds, *IEEE Trans. Antennas Propagat.*, **AP-29**:455-462.

8. Hung, C.C. and Mittra, R. (1983) Secondary pattern and focal region distribution of reflector antennas under wide-angle scanning, *IEEE Trans. Antennas Propagat.*, **AP-31**:756-763.

9. Rinous, P.J., et al (1983) The analysis of hybrid reflector antennas, *Third International Conference on Antennas and Propagation ICAP 83*, pp. 318-321.

10. O'Brien, M.J., and Shore, R.A. (1984) Paraboloid scanning by array feeds: a low sidelobe synthesis technique, *IEEE AP-S International Symposium, 1984 International Symposium Digest, Antennas and Propagation, Vol. I*, pp. 272-275.

11. Pearson, R.A., et al (1986) Electronic beam scanning using an array-fed dual offset reflector antenna, *IEEE AP-S International Symposium, 1986 International Symposium Digest, Antennas and Propagation, Vol. I*, pp. 263-266.

12. Scott, W.G., et al (1977) Design tradeoffs for multibeam antennas in communication satellites, IEEE Communications Society Magazine, **15**:(No. 2)9-15.

13. Bird, T.S. (1982) Contoured-beam synthesis for array-fed reflector antennas by field correlation, *IEE Proc.*, 129:(Pt. H)293-298.

14. Ricardi, L.J. (1982) Multiple beam antennas, *The Handbook of Antenna Design, Vol. 1*, A.W. Rudge et al, Eds., Peter Peregrinus, Ltd., London, Chap. 6.

15. Balling, P. (1987) Spacecraft multi-beam and contoured-beam antennas, *AGARD Lecture Series No. 151, Microwave Antennas for Avionics.*

16. Adatia, N., et al (1989) Multicoverage shaped reflector antenna designs, *IEEE International Symposium, 1989 International Symposium Digest, Antennas and Propagation, Vol. 3*, pp. 1182-1186.

17. Bird, T.S., and Boomars, J.L. (1980) Evaluation of focal fields and radiation characteristics of a dual-offset reflector antenna, *IEE Proc.*, **127**:(Pt. H)209-218.

18. Hsaio, J.K. (1983) *A FORTRAN Computer Program to Compute the Radiation Pattern of an Array-Fed Paraboloidal Reflector*, Naval Research Laboratory Report 8740.

19. Morris, G. (1984) Receiving analysis of the shaped cylindrical reflector antenna with an array feed, *IEE Proc.*, **131**:(Pt. H)123-125.

20. Steyskal, H. and Shore, R.A. (1984) *Efficient Computation of Reflector Antenna Aperture Distributions and Far Field Patterns*, Rome Air Development Center Rept. RADC-TR-84-45, Available from National Technical Information Service (NTIS) AD A143319.

21. Jong, H.Y., et al (1984) Analysis of paraboloidal reflector fields under oblique incidence, *IEEE International Symposium, 1984 International Symposium Digest, Antennas and Propagation*, Vol. 1, pp. 305-308.

22. Clarricoats, P.J.B., et al (1984) Effects of mutual coupling in conical horn arrays, *IEE Proc.*, **131**:(Pt. H)165-171.

23. Clarricoats, P.J.B., et al (1984) Performance of offset reflector antennas with array feeds, *IEE Proc.*, **131**:(Pt. H)172-178.

24. Lam, P.T., et al (1985) Directivity optimization of a reflector antenna with cluster feeds: a closed form solution, *IEEE Trans. Antennas Propagat.*, **AP-33**:1163-1174.

25. Rusch, W.V.T., and Prata, A. (1990) *Computation of Focal-Region Fields of Offset Dual Reflector Antennas for Scanning Applications*, Rome Air Development Center Rept. RADC-TR-90-299, AD B153991L.

26. Rusch, W.V.T., and Prata, A. (1991) *Efficient Computation of Classical Offset Dual Reflector Antennas Excited by Array Feeds*, Rome Laboratory Rept. RL-TR-91-7, AD B154936L.

27. Chadwick, G.G., et al (1980) Adaptive antenna/receiver-processor system, *Proceedings of the 1980 Antenna Applications Symposium, Robert Allerton Park, University of Illinois.*

28. Chadwick, G.G., et al (1981) Adaptive antenna/receiver processor system, *IEEE-AP-S-International Symposium, 1981 International Symposium Digest, Antennas and Propagation*, Vol. I, pp. 272-275.

29. Mayhan, J.T. (1976) Nulling limitations for a multiple-beam antenna, *IEEE Trans. Antennas Propagat.*, **AP-24**:769-779.

30. Mayhan, J.T. (1978) Adaptive nulling with multiple-beam antennas, *IEEE Trans. Antennas Propagat.*, **AP-26**:267-273.

31. Mayhan, J.T. (1979) Some techniques for evaluating the bandwidth characteristics of adaptive nulling systems, *IEEE Trans. Antennas Propagat.*, **AP-27**:363-373.

32. Jim, C.W. (1977) A comparison of two LMS constrained optimal array structures, *Proc. IEEE*, **65**:1730-1731.

33. Griffiths, L.J., and Jim, C.W. (1982) An alternative approach to linearly constrained adaptive beamforming, *IEEE Trans. Antennas Propagat.*, **AP-30**:27-34.

34. Griffiths, L.J., and Buckley, K.M. (1987) Quiescent pattern control in linearly constrained adaptive arrays, *IEEE Trans. Acoustics, Speech, and Signal Processing*, **ASSP-35**: 917-926.

35. Widrow, B., et al (1967) Adaptive antenna systems, *Proc. IEEE*, **55**:2143-2159.

36. Rao, C.R., and Mitra, S.K. (1971) *Generalized Inverse of Matrices and Its Applications*, John Wiley, New York, Chap. 3.

37. Trudnowski, D.J. (1988) *Adaptive Array Beamforming Using the Generalized Sidelobe Canceller*, Electronic Research Laboratory, Rept. No. 188, Montana State University, Bozeman, MT 59717.

38. Rahmat-Samii, Y. (1988) Reflector antennas, *Antenna Handbook*, Y.T. Lo and S.W. Lee, Eds., Van Nostrand Reinhold, New York, Chap. 15.

39. Ludwig, A.C. (1973) The definition of cross polarization, *IEEE Trans. Antennas Propagat.*, **AP-21**:116-119.

MISSION

OF

ROME LABORATORY

Rome Laboratory plans and executes an interdisciplinary program in research, development, test, and technology transition in support of Air Force Command, Control, Communications and Intelligence (C^3I) activities for all Air Force platforms. It also executes selected acquisition programs in several areas of expertise. Technical and engineering support within areas of competence is provided to ESD Program Offices (POs) and other ESD elements to perform effective acquisition of C^3I systems. In addition, Rome Laboratory's technology supports other AFSC Product Divisions, the Air Force user community, and other DOD and non-DOD agencies. Rome Laboratory maintains technical competence and research programs in areas including, but not limited to, communications, command and control, battle management, intelligence information processing, computational sciences and software producibility, wide area surveillance/sensors, signal processing, solid state sciences, photonics, electromagnetic technology, superconductivity, and electronic reliability/maintainability and testability.